

## Glycosphingolipids in cestodes

### Chemical structures of ceramide monosaccharide, disaccharide, trisaccharide and tetrasaccharide from metacestodes of the fox tapeworm, *Taenia crassiceps* (Cestoda: Cyclophyllidae)

Roger D. DENNIS<sup>1</sup>, Stefan BAUMEISTER<sup>2</sup>, Rudolf GEYER<sup>3</sup>, Jasna PETER-KATALINIC<sup>4</sup>, Rudolf HARTMANN<sup>4</sup>, Heinz EGGE<sup>4</sup>, Egbert GEYER<sup>2</sup> and Herbert WIEGANDT<sup>1</sup>

<sup>1</sup> Institut für Physiologische Chemie der Universität Marburg, Federal Republic of Germany

<sup>2</sup> Fachbereich Biologie der Universität Marburg, Federal Republic of Germany

<sup>3</sup> Institut für Biochemie der Universität Giessen, Federal Republic of Germany

<sup>4</sup> Institut für Physiologische Chemie der Universität Bonn, Federal Republic of Germany

(Received December 23, 1991/May 22, 1992) – EJB 91 1722

The presence of glycosphingolipids in the metacestodes of the fox tapeworm, *Taenia crassiceps*, has been established. The normal-phase TLC pattern of the neutral-fraction glycolipids revealed groups of bands corresponding to homologous components of increasing sugar chain length. The three simplest glycolipid components have been isolated and their chemical constitution determined as being of the neogala series: Gal $\beta$ 1Cer, Gal $\beta$ 6Gal $\beta$ 1Cer and Gal $\beta$ 6Gal $\beta$ 6Gal $\beta$ 1Cer. The ceramide tetrasaccharide fraction has been found to consist of a mixture of neogalatetraosylceramide, as an elongation of the neogala series, Gal $\beta$ 6Gal $\beta$ 6Gal $\beta$ 6Gal $\beta$ 1Cer and the component Gal $\alpha$ 4Gal $\beta$ 6Gal $\beta$ 6Gal $\beta$ 1Cer (both occurring in approximately equimolar proportions). The long-chain bases of the ceramide monogalactoside, digalactoside, trigalactoside and tetragalactosides contain, as well as small amounts of sphingosine, predominantly dihydrosphingosine/phytosphingosine in the approximate ratios 1.7:1, 1.4:1, 1:1 and 2.3:1, respectively. The major ceramide fatty acids have particularly long chains, with hexacosanoic and octacosanoic acids predominating. Upon reverse-phase TLC, the glycolipid components ceramide monogalactoside, digalactoside and trigalactoside were each separable into five component bands. Parent glycolipid components therefore show component band distributions comparable to one another in being governed by similar ceramide constitutions.

As a possible reflection of their general relevance in biology, glycolipids are widely distributed in tissues of plants [1, 2], animals [3] and microorganisms [4]. Amongst the glycolipids, the glycosphingolipids have attracted particular attention because of their involvement in the modulation of cellular growth and differentiation behaviour [5–7], binding to cytoskeletal elements [8, 9], combined intracellular transport of protein/glycosphingolipid complexes [10] and expression of the immune characteristics of cells [11]. Whereas the ceramide (Cer) moieties, i.e. the lipophilic domains, of glycosphingolipids appear to be similar to each other, the single sugars, and more so their oligosaccharide chains, constitute a repertoire of remarkably variable configurations of still unknown biological significance. It presents a particular challenge to the contemporary biochemist to give an explanation this large structural diversity of glycosphingolipids.

Correspondence to H. Wiegandt, Institut für Physiologische Chemie der Philipps-Universität Marburg, Karl von Frisch-Strasse, Lahnberge, W-3550 Marburg 18, Federal Republic of Germany

Fax: +49 6421 286957.

Abbreviations. CMH, ceramide monohexoside; CDH, ceramide dihexoside; CTetH, ceramide tetrahexoside; CTH, ceramide trihexoside; FAB, fast atom bombardment; 26:0, hexacosanoic acid; 28:0, octacosanoic acid; 30:0, decacosanoic acid; Hex, hexose; HH-COSY, homonuclear, chemical-shift correlation spectra; Cer, ceramide.

Enzymes.  $\alpha$ -D-Galactoside galactohydrolase (EC 3.2.1.22);  $\beta$ -D-galactoside galactohydrolase (EC 3.2.1.23).

An investigation of the glycolipids of multicellular parasites (protozoan parasites do not appear to contain major amounts of classical glycosphingolipids, i.e. compounds containing sugar linked to ceramide) was initiated in this laboratory, with the aim of increasing our knowledge of the diversity and distribution of their glycosphingolipids. It is hoped that this information will contribute to a better understanding of the putative roles of parasite glycosphingolipids in the maintenance of parasite integrity, in the mediation of parasite/host interactions and in their significance in the host immune response. As a model, the metacestode stage of *Taenia crassiceps* has been chosen because of its relevance to other parasitic helminths that are pathogenic in humans, as well as for ease of propagation in laboratory mice [12]. Preliminary data have shown their neutral-fraction glycolipids to be antigenic, as evidenced by immunoreactivity (ELISA and HPTLC immunostaining) towards *T. crassiceps* metacestode-elicited infection serum, and, interestingly, against an affinity-column-isolated fraction [with parasite-derived ceramide trihexoside (CTH) as the ligand] [13].

The results have shown that *T. crassiceps* metacestodes contain an array of glycolipids which can be separated by TLC into groups of chromatographic bands corresponding to homologous components of increasing sugar chain length. Isolation of ceramide monosaccharide, disaccharide, trisaccharide and tetrasaccharides has allowed their structural characterisation as members of the neogala series. Glyco-

sphingolipids with carbohydrate moieties identical to those of the metacestodes have been previously identified by Matsubara and Hayashi as being restricted to various archaeogastropod marine snails [14, 15].

## MATERIALS AND METHODS

*T. crassiceps* metacestodes were reared in NMRI mice for 80 days, harvested, washed repeatedly and consecutively in isotonic saline and deionised water prior to lyophilisation. The organic solvents used were of the highest purity available. DEAE-Sephadex A-25 was from Pharmacia (Freiburg); exoglycosidases and selected fatty acid, long-chain-base and monosaccharide standards were from Sigma (Deisenhofen); normal-phase and reverse-phase (RP-18) HPTLC<sub>60</sub> silica-gel plates, butyllithium and Florisil were from Merck (Darmstadt); methyl iodide was from Roth (Karlsruhe); selected monosaccharide standards were from Fluka (Neu-Ulm); selected fatty-acid standards and sodium borohydride were from Serva (Heidelberg); *N,N*-dimethylformamide dimethyl acetal and *N*-methyl-*N*-(trimethylsilyl)trifluoroacetamide were from Macherey-Nagel (Düren); normal-phase and reverse-phase (C<sub>18</sub>) Sep-Pak silica-gel cartridges were purchased from Waters Millipore (Eschborn). C<sup>2</sup>HCl<sub>3</sub> (100 <sup>2</sup>H/100 H atom) for NMR spectroscopy was obtained from Aldrich (Steinheim).

### Isolation, purification and separation of individual neutral-fraction glycolipids

The lyophilised metacestodes of *T. crassiceps* (20 g) yielded 350 mg isolated, total neutral-fraction glycolipids [16]. Individual glycolipid components or glycolipid component bands were separated and obtained by preparative HPTLC on either normal-phase plates, at a loading of approximately 500 µg/plate and running solvent, chloroform/methanol/water (65:25:4, by vol.), or reverse-phase plates and resolved, by duplication (four times), with the running solvent methanol/acetonitrile/water (19:5:1, by vol.) at 32°C [17]. The glycolipids were routinely detected by orcinol/H<sub>2</sub>SO<sub>4</sub> (0.2% orcinol in 2 M H<sub>2</sub>SO<sub>4</sub>) at 110°C for 5 min. The reverse-phase plates required prior treatment with 70% ethanol. The relevant glycolipid-containing bands were scraped from the plate, eluted with 2-propanol/*n*-hexane/water (55:20:25, by vol.; lower layer employed) and filtered (type HV, 0.45 µm pore size, Nihon Millipore, Kogyo).

### Analysis of fatty acids and long-chain bases

The purity of long-chain base standards was tested by normal-phase HPTLC with the running solvent chloroform/methanol/25% aqueous ammonia (100:25:2.5, by vol.) [18] and visualised using a ninhydrin spray reagent at 100°C for 3 min. The glycolipids (100 µg) were hydrolysed, according to Gaver and Sweeley [19], with the procedure of Hanfland [20] for the separation of fatty-acid-containing and long-chain-base-containing fractions and simultaneous removal of carbohydrate residues. The fatty acids, derivatised as their *O*-methyl esters, were analysed by capillary GC (Carlo Erba HRGC 5160 gas chromatograph) on a DB-1701 fused-silica, bonded-phase column (Carlo Erba, Hofheim; 30 m, linear temperature gradients of 60–80°C at 4°C/min and 80–220°C at 2°C/min, and isothermal for 20–35 min depending on fatty-acid chain length). Likewise, the long-chain bases, derivatised

as their trimethylsilyl ethers, were separated on a DB-225 column (Carlo Erba, Hofheim; 30 m, linear temperature gradients of 100–120°C at 4°C/min and 120–220°C at 3°C/min, and isothermal for 20 min). The putative presence of 2-hydroxy fatty acids was determined by acetylation of the fatty-acid methyl esters [20]. For confirmation of the long-chain bases and major fatty acids detected, the same sample(s) was subjected to capillary GC/MS with a LKB 9000 GC mass spectrometer, at 20 eV ionisation energy, on a fused-silica column BP1 (25m; SGE, Australia) and helium as carrier gas. The common temperature programme was 150–315°C at 5°C/min followed, when necessary, isothermally for 15 min at 315°C.

Prior to the analysis of glycolipid component bands isolated from reverse-phase HPTLC<sub>60</sub> plates, it was necessary to remove introduced contaminants by Sep-Pak cartridges, in the following sequence: normal-phase, washed with chloroform/methanol (98:2) and eluted with chloroform/methanol/water (60:35:8, by vol.); reverse-phase, washed with distilled water and methanol/water (1:1, by vol.) and eluted with methanol and chloroform/methanol/water (65:25:4 and 60:35:8, by vol.) [21].

### Carbohydrate-component and methylation analysis

TLC identification of monosaccharides present in glycolipids (75 µg) was performed subsequent to a two-step hydrolysis by 1.0 M methanolic HCl/water (82:18, by vol.) at 70°C for 24 h, evaporation to dryness and 1.0 M HCl at 100°C for 60 min, before evaporation, combining the methods of Gaver and Sweeley [19] and Kuhn and Wiegandt [22]. Following Folch partition, the monosaccharide-containing fraction was separated into component sugars on normal-phase plates, twice with the running solvent pyridine/ethyl acetate/acetic acid/water (3:5:1:2, by vol.) and visualisation by orcinol/H<sub>2</sub>SO<sub>4</sub>.

For monosaccharide-constituent analysis, glycolipids (50 µg) were hydrolysed with 500 µl 0.25 M H<sub>2</sub>SO<sub>4</sub> in 85% acetic acid at 80°C for 16 h, and the sugar components derivatised as their alditol acetates [23]. The derivatives were analysed by capillary GC on either fused-silica, bonded-phase columns (Carlo Erba, Hofheim; DB-1 60 m and DB-210 30 m, linear temperature gradient of 100–250°C at 2°C/min) or a WCOT glass column (Carlo Erba, Hofheim; OV1 60 m, linear temperature gradient 100–250°C at 3°C/min).

Likewise, for carbohydrate-constituent-linkage-position analysis, glycolipids (50 µg) were permethylated [24, 25], hydrolysed and the sugar components analysed as their partially methylated alditol acetates. The derivatives were studied by GC on DB-1 and DB-210 capillary columns or by GC/MS on a DB-1 capillary column [23]. The sodium methylsulphonyl carbanion has been replaced in this procedure by lithium methylsulphonyl carbanion because of the increased purity [26].

### Exoglycosidase treatment

This was performed [27] with 10 µg glycolipid in 100 µl 0.05 M sodium citrate containing 0.1% sodium taurodeoxycholate at 37°C for 21 h and treated, either with  $\alpha$ -galactosidase (*Coffea arabica*, two additions of 0.2 U) at pH 6.0 or  $\beta$ -galactosidase (*Canavalia ensiformis*, two additions of 0.05 U) at pH 4.0. Cleavage was monitored by TLC. Addition of 10 mM  $\beta$ -galactosidase inhibitor  $\gamma$ -galactonolactone [28] reduced this side activity in the  $\alpha$ -galactosidase



Fig. 1. TLC analysis of neutral-fraction glycolipids from *T. crassiceps* metacestodes. TLC: HPTLC<sub>60</sub> plates; running solvent, chloroform/methanol/water (65:25:4, by vol.); spray reagent, orcinol/H<sub>2</sub>SO<sub>4</sub>. S, *T. crassiceps* total neutral glycolipid fraction; H, human spleen total neutral glycolipid fraction; C, *C. vicina* total neutral glycosphingolipid fraction; 1–4, rechromatography of isolated glycolipid components 1–4.

preparation (in 0.2 U of the *C. arabica* enzyme 5%  $\beta$ -galactosidase activity under the same conditions of glycolipid cleavage) by 70%.

#### Fast-atom bombardment (FAB)-MS

MS was accomplished on a VG-ZAB HF mass spectrometer (V. G. Analytical, Manchester) equipped with an Ion-Tech gun [29], native glycolipids being examined in both the negative- and positive-ion modes. The glycolipids (5  $\mu$ g), dissolved in chloroform/methanol (1:1, by vol.), were applied to the matrix of triethanolamine or thioglycerol on the target and bombarded with xenon atoms at a kinetic energy equivalent to 9 keV.

#### <sup>1</sup>H-NMR spectroscopy

Peracetylated glycolipids ( $\geq 200$   $\mu$ g) in 0.5 ml C<sup>2</sup>HCl<sub>3</sub> were scanned and the 500-MHz spectrum recorded at 303 K on a Bruker AMX-500 spectrometer with a X-32 computer and standard Bruker software. The spectral width was 4 kHz with 16 K data points; 21 800 scans were accumulated for ceramide dihexoside (CDH) and 18 500 for ceramide trihexoside (CTH). Before Fourier transformation, the free induction decays were multiplied with a Gaussian function (line broadening =  $-1$ ; Gaussian broadening = 0.2) and zero-filled to 32 K data points. For two-dimensional, homonuclear, chemical-shift correlation spectra (HH-COSY) [30] the time-domain matrix comprised 2 K data points in  $t_2$  and 256 data points in  $t_1$  (512 scans/ $t_1$ ). The matrix was zero-filled in  $t_1$  to 2 K data points and multiplied in both dimensions with a square sinus function (SSB = 0) and Fourier transformed. Phase correction was achieved by squaring of the signal amplitude.

## RESULTS

#### Isolation and TLC analysis

The major step in the isolation of the four simplest neutral glycolipids was preparative HPTLC. The following component bands were discernible according to HPTLC (Fig. 1): component 1, three constituent bands of  $R_F$  0.78; component 2, five constituent bands of  $R_F$  0.54; component 3, five constituent bands of  $R_F$  0.29; component 4, five constituent bands

of  $R_F$  0.18 ( $R_F$  was determined from the migration properties of the main constituent band of each component). The neutral glycolipid fraction is complex, consisting of at least 18 orcinol/H<sub>2</sub>SO<sub>4</sub>-positive bands (Fig. 1). However, at least for the glycolipids covered by the present investigation, the component bands are grouped together and, by comparison of their running properties with co-migrating standards of known structure, component 1 represents a monohexosyl glycolipid, component 2 a dihexosyl glycolipid, component 3 a trihexosyl glycolipid and component 4 a tetrahexosyl glycolipid. The multiple component bands observed for each putative neutral glycolipid species, as opposed to the single component bands of each *Calliphora vicina* neutral glycosphingolipid standard (Fig. 1, lane C) [16, 31], may be interpreted as being due to the heterogeneity of their lipid moieties.

#### Ceramide analysis

The putative glycolipid components 1–4 were separated into their constituent TLC component bands by reverse-phase HPTLC (migration according to molecular hydrophobic, not hydrophilic, properties), reisolation of the component bands and rechromatography on normal-phase HPTLC plates (Fig. 2). Each component could be separated into five TLC constituent bands. Each neutral glycolipid component (1–4), as well as selected reverse-phase isolated component bands (those available in sufficient quantity for chemical analysis), were then analysed for the long-chain base and fatty-acid content of their ceramide moieties.

The long-chain base compositions of glycolipid components 1–4 were analysed as their trimethylsilyl derivatives and their percentage distributions are given in Table 1. They are characterised by a preponderance of dihydrosphingosine and phytosphingosine. The constitutions of selected individual component bands are also presented in Table 1, where either phytosphingosine, dihydrosphingosine or a combination of the two are the usual dominant long-chain base species present.

The distributions of fatty acids in the same glycolipid components (Fig. 3) and component bands (Table 2) were investigated, analysed as their methyl esters and characterised by the presence of very-long-chain species, i.e. hexacosanoic acid (26:0) and octacosanoic acid (28:0) as the major class, and the absence of  $\alpha$ -hydroxy fatty acids (data not shown). In addition, there is a repetition of certain fatty acids in the selected component bands; the intermediate migrating species (M3, D3, T3 and Q3) express a relatively even distribution of fatty acids, whilst the more rapidly migrating species (M5, D5, T5 and Q5) show a predominance of the very-long-chain type; i.e. 26:0 and 28:0. The identification of the lipid moieties as ceramide allows the use of the designation glycosphingolipid for these components.

#### Carbohydrate constituent and methylation analysis

TLC analysis of the monosaccharide constituent(s) of glycosphingolipid components 1–4 suggested the sole presence of galactose (data not shown). This was confirmed by determination as its alditol acetate, where glucose was present in minor amounts not exceeding 3.5% that of galactose (data not shown). Methylation analysis of component 1 revealed the sole presence of terminal galactose. Trace amounts of terminal glucose were also detected. Components 2 and 3 were found to comprise one terminal and one or two C6-substituted galactose residues, respectively, demonstrating 1–6 link-

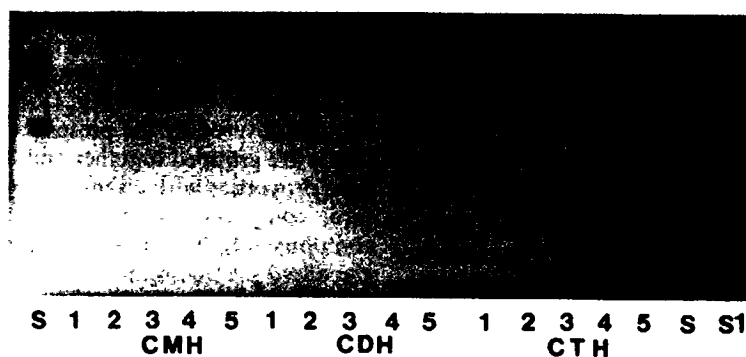


Fig. 2. Normal-phase TLC analysis of reverse-phase HPTLC<sub>60</sub>-isolated neutral-fraction glycolipid component bands from *T. crassiceps* metacystodes. TLC: HPTLC<sub>60</sub> plates; running solvent, chloroform/methanol/water (65:25:4, by vol.); spray reagent, orcinol/H<sub>2</sub>SO<sub>4</sub>. S, human spleen CMH and CDH; S1, total neutral-glycolipid fraction of *T. crassiceps* metacystodes. Rechromatography of RP-18 HPTLC<sub>60</sub>-isolated neutral-fraction glycolipid component bands on normal-phase HPTLC<sub>60</sub> plates: 1–5 (CMH), from glycolipid component 1; 1–5 (CDH), from glycolipid component 2; 1–5 (CTH), from glycolipid component 3.

Table 1. Long-chain base composition of *T. crassiceps* glycolipid components 1–4 and reverse-phase-isolated HPTLC component bands. Glycolipid component HPTLC bands: M, monohexosyl; D, dihexosyl; T, trihexosyl; Q, tetrahexosyl; see Fig. 2 for classification of HPTLC component bands.

Long-chain base	Amount in component				Amount in component bands									
	1	2	3	4	M1	M3	M4	M5	D3	D5	T3	T5	Q3	Q5
	% total													
Sphingosine (18:1)	0.5	0.2	2.0	0.9	–	–	43.0	–	–	–	–	–	–	–
Dihydrosphingosine (18:0)	63.2	58.4	48.8	69.8	–	99.1	30.5	34.1	100.0	48.0	100.0	36.5	100.0	63.8
Phytosphingosine (18:0)	36.3	41.4	49.1	29.4	100.0	0.9	26.5	65.9	–	52.0	–	63.5	–	36.2

age(s). In addition to the terminal and C6-substituted galactose species, component 4 contained a second species with a C4-substituted galactose, indicating an oligosaccharide chain with one (1–4)Gal residue. The numerical data for these conclusions are summarised in Table 3.

#### Exoglycosidase analysis

Glycosphingolipid component 1 was refractory to cleavage on treatment with either  $\alpha$ -galactosidase or  $\beta$ -galactosidase (Fig. 4, lanes B and C, respectively). The terminal galactose residue of glycosphingolipid components 2 and 3 was shown to be  $\beta$ -linked, as cleavage was evident only on incubation with  $\beta$ -galactosidase (Fig. 4, lanes F and I, respectively). The terminal galactose residue of glycosphingolipid component 4 was cleaved by both  $\alpha$ -galactosidase and  $\beta$ -galactosidase (Fig. 4, lanes K and L and O, respectively). This result is interpreted as being due to the presence of two oligosaccharide species. The terminal galactose of the faster-migrating fraction of component 4 (Fig. 4, lane J) is present in the  $\alpha$ -anomeric configuration of one species (Fig. 4, lane K) and in the  $\beta$  conformation of the other (Fig. 4, lane L). In contrast, the terminal galactose of the slower-migrating fraction of component 4 (Fig. 4, lane M) occurs solely in a  $\beta$  configuration (Fig. 4, lane O). This conclusion is corroborated by the result of methylation analysis of the slower-migrating fraction of component 4 (data not shown), which demonstrated the presence of only one terminal and three C6-substituted galactosyl residues. A further observation was that the terminal  $\beta$ -galactose-containing components 3 and 4 were completely

cleaved by  $\beta$ -galactosidase to monosaccharide and ceramide because of the absence of component 1 (Fig. 4, lanes I, L and O); the terminal  $\alpha$ -galactose-containing component 4 was cleaved by  $\alpha$ -galactosidase to component 3, i.e. removal of a single sugar residue (Fig. 4, lane K). We have no explanation at present for the phenomenon of component-1  $\beta$ -galactosidase refractoriness, except for its apparent cleavage as an intermediate during cleavage of components 3 and 4.

#### FAB-MS

Glycosphingolipid component 1 was represented in negative-ion FAB-MS by the pseudomolecular (M-H)<sup>–</sup> ions at  $m/z$  700 Da (major) and the 16-Da-greater constituent at  $m/z$  716 Da, beside the corresponding chloride adduct ions at  $m/z$  736 Da and 752 Da. The type of monosaccharide present, deduced by the mass difference between the two ceramide anions (Cer-O)<sup>–</sup> at  $m/z$  538 Da and 554 Da and the respective pseudomolecular (M-H)<sup>–</sup> ions, was hexose (Hex; 162 Da; Figs 5a and 8a).

The minor ion at  $m/z$  554 Da, an increase of 16 Da over that of the major one, was provisionally attributed to a hydroxylated ceramide species. The occurrence of palmitic acid as the major fatty-acid residue detected and dihydrosphingosine and phytosphingosine as the main long-chain bases was determined in the positive-ion FAB-MS from the (M + 2H<sup>+</sup> - acyl)<sup>+</sup> ions at  $m/z$  464 Da and 480 Da (Figs 6a and 8b) [32].

The negative-ion FAB-MS of minor amounts of the pseudomolecular ions at  $m/z$  840 Da and 856 Da indicate the existence of ceramide species containing a 26:0 fatty-acid

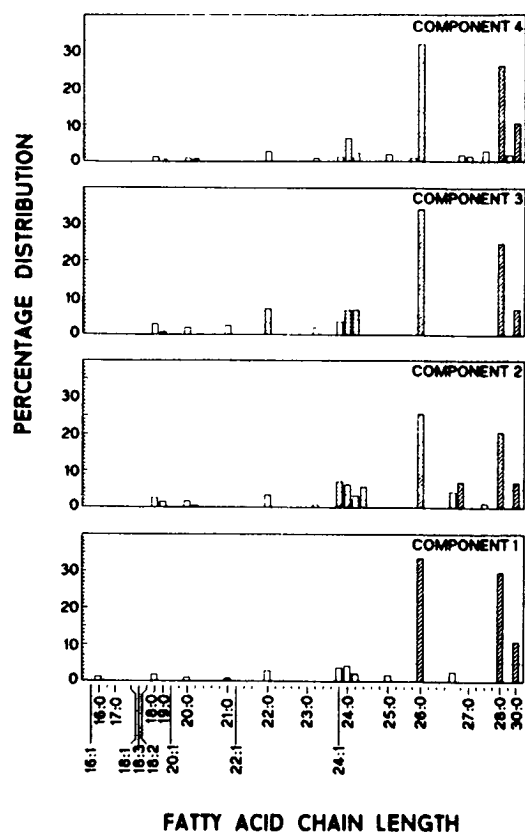


**Fig. 3. Fatty-acid composition of *T. crassiceps* glycolipid components 1–4.** Fatty acids were analysed as their methyl esters by capillary GC. The percentage distribution of fatty acids is depicted in the form of a bar diagram with computation of all peaks greater than 1% of total; those greater than 5% of total were taken as significant and are represented by hatched bars. Two non-fatty-acid peaks with retention times of 67.7 min and 69.3 min were also detected; the latter was identified by capillary GC/MS as the plasticiser dioctyl phthalate. 16:0, hexadecanoic acid; 16:1, hexadecenoic acid; 18:0, octadecanoic acid; 18:1, octadecenoic acid; 18:2, octadecadienoic acid; 18:3, octadecatrienoic acid; 19:0, nonadecanoic acid; 20:0, icosanoic acid; 21:0, unicosanoic acid; 22:0, docosanoic acid; 22:1, docosenoic acid; 23:0, tricosanoic acid; 24:0, tetracosanoic acid; 24:1, tetracosenoic acid; 25:0, pentacosanoic acid; 27:0, heptacosanoic acid.

residue. This was confirmed with the reverse-phase-HPTLC-isolated component band 5, derived from glycosphingolipid component 1 (see Fig. 2 for HPTLC component band classification). In addition to the pseudomolecular ions of  $m/z$  840 Da and 856 Da, which represent 26:0 with dihydrosphingosine and phytosphingosine, respectively, the ions at  $m/z$  868 Da and 884 Da corresponded to 28:0 fatty acid with the same respective long-chain bases (Fig. 7).

The pseudomolecular ( $M+H$ )<sup>+</sup> ions were at  $m/z$  702 Da and 718 Da, and protonated ceramide moieties (CerOH·H)<sup>+</sup> at  $m/z$  540 Da and 556 Da which, on elimination of H<sub>2</sub>O, yielded Cer<sup>+</sup> at  $m/z$  = 522 Da and 538 Da. The absence of long-chain base cations in positive-ion FAB-MS is in accord with the structural requirements necessary for their formation, i.e. the existence of a double bond at C4 (Figs 6a and 8b) [32].

The pseudomolecular ( $M-H$ )<sup>−</sup> ions of glycosphingolipid component 2 in negative-mode FAB-MS were at  $m/z$  862 Da and 878 Da (chloride adducts at  $m/z$  898 Da and 914 Da); the 16-Da difference relating to ceramide species with the long-chain bases dihydrosphingosine and phytosphingosine, respectively. The carbohydrate sequence of Hex-Hex was cor-

**Table 2. Fatty-acid composition of *T. crassiceps* selected reverse-phase-HPTLC-isolated component bands.** Capillary GC peaks were specified either as identified fatty acids or from retention time (min) shown in parentheses. For definitions of abbreviations, see the legends to Table 1 and Fig. 3. The values are percentage distribution of fatty acids with computation of all peaks greater than 4% of total; those 15% of total were taken as significant and are shown in bold type.

Fatty acid or retention time	Amount in component band									
	M1	M3	M4	M5	D3	D5	T3	T5	Q3	Q5
	% total									
16:0	—	8.9	—	—	8.3	—	—	—	—	—
(44.25)	—	—	—	—	7.5	—	—	—	—	—
18:0	<b>20.3</b>	<b>15.6</b>	10.3	—	13.5	7.6	<b>22.8</b>	12.9	<b>43.8</b>	<b>15.2</b>
20:0	6.8	—	8.0	—	—	—	10.5	—	8.4	—
(58.48)	—	—	—	—	—	—	—	—	—	10.5
21:0	<b>15.4</b>	—	—	—	—	—	9.7	—	—	—
22:1	—	—	—	—	—	—	13.4	4.6	14.3	—
(64.97)	—	<b>22.9</b>	13.4	—	—	6.7	5.6	—	—	—
(65.31)	12.5	—	—	—	—	—	—	—	—	—
22:0	—	—	9.8	—	12.8	<b>16.6</b>	—	—	—	—
(72.08)	9.6	—	—	—	—	—	—	—	—	—
24:1	—	—	5.2	—	—	—	—	—	—	—
24:0	7.6	10.0	11.7	7.7	—	5.6	—	9.1	9.0	6.7
(75.28)	—	—	—	—	8.2	—	—	—	—	—
(75.68)	12.5	8.7	11.9	—	—	—	—	—	—	—
25:0	4.0	—	—	—	—	—	—	—	4.4	—
(78.11)	—	—	—	—	14.0	—	—	—	—	—
26:0	—	<b>20.6</b>	<b>15.5</b>	<b>49.5</b>	—	<b>34.9</b>	—	<b>42.6</b>	—	<b>33.0</b>
(83.42)	—	—	—	—	9.1	—	—	—	—	—
(84.25)	—	—	6.0	—	—	—	—	—	—	—
27:0	—	—	—	—	<b>26.7</b>	—	<b>38.1</b>	—	<b>20.1</b>	—
(90.36)	7.3	—	8.5	—	—	—	—	—	—	—
(92.85)	—	12.9	—	—	—	—	—	—	—	—
28:0	—	—	—	<b>43.1</b>	—	<b>28.9</b>	—	<b>30.5</b>	—	<b>34.2</b>

**Table 3. Methylation analysis of *T. crassiceps* glycolipid components 1–4.** Results are mean values of capillary GC/capillary GC/MS. 2,3,4,6-GalOH, etc., 2,3,4,6-tetra-*O*-methyl-D-galactitol, etc.

Alditol acetate	Peak ratio of component				Linkage
	1	2	3	4	
2,3,4,6-GalOH	0.97 <sup>a</sup>	1.0 <sup>b</sup>	1.0 <sup>b</sup>	1.0 <sup>b</sup>	terminal
2,3,4-GalOH	—	1.15	2.15	2.8	C6 substituted
2,3,6-GalOH	—	—	—	0.5	C4 substituted
2,3,4,6-GlcOH	0.03 <sup>a</sup>	—	—	—	terminal

<sup>a</sup> Based on 2,3,4,6-GalOH and 2,3,4,6-GlcOH

<sup>b</sup> Based on 2,3,4,6-GalOH

roborated by the ions ( $M-H$ -Hex)<sup>−</sup> at  $m/z$  700 Da and 716 Da and (Cer-O)<sup>−</sup> at  $m/z$  538 Da and 554 Da (Figs 5b and 8a). The pseudomolecular ( $M+H$ )<sup>+</sup> ions in positive-ion FAB-MS were at  $m/z$  864 Da and 880 Da. The ceramide moiety, deduced from the ions ( $M+2H^+$ -acyl)<sup>+</sup> at  $m/z$  626 Da and 642 Da, as well as Cer<sup>+</sup> and (CerOH·H)<sup>+</sup> at  $m/z$  522/538 Da and 540/556 Da, respectively, was ascertained to contain palmitic acid as fatty-acid residue and dihydrosphingosine and phytosphingosine as the main long-chain bases, in agreement with that for glycosphingolipid component 1 (Figs 6b and 8b).

The pseudomolecular ( $M-H$ )<sup>−</sup> ions of glycosphingolipid component 3 in negative-mode FAB-MS were at  $m/z$  1024 Da



**Fig. 4.** TLC of glycolipid components 1–4 following exoglycosidase treatment. Incubated and extracted glycolipids were separated with running solvent chloroform/methanol/water (65:25:4, by vol.) and visualised with orcinol/ $\text{H}_2\text{SO}_4$ . The arrow marks sodium taurodeoxycholate spot. S, total neutral-fraction glycolipids of *T. crassiceps* metacestodes; A, component 1 untreated; B, component 1 with  $\alpha$ -galactosidase; C, component 1 with  $\beta$ -galactosidase; D, component 2 untreated; E, component 2 with  $\alpha$ -galactosidase; F, component 2 with  $\beta$ -galactosidase; G, component 3 untreated; H, component 3 with  $\alpha$ -galactosidase; I, component 3 with  $\beta$ -galactosidase; J, component 4<sub>f</sub> (fast-migrating component bands) untreated; K, component 4<sub>f</sub> with  $\alpha$ -galactosidase; L, component 4<sub>f</sub> with  $\beta$ -galactosidase; M, component 4<sub>s</sub> (slow-migrating component bands) untreated; N, component 4<sub>s</sub> with  $\alpha$ -galactosidase; O, component 4<sub>s</sub> with  $\beta$ -galactosidase.

and 1040 Da, accompanied by chloride adducts at  $m/z$  1060 Da and 1076 Da. The carbohydrate sequence Hex-Hex-Hex was derived from the ion pairs, each segregated by 16 Da:  $m/z$  862 Da and 878 Da ( $\text{M-H-Hex}^-$ );  $m/z$  700 Da and 716 Da ( $\text{M-H-2Hex}^-$ );  $m/z$  538 Da and 554 Da ( $\text{Cer-O}^-$ ) (Figs 5c and 8a). In positive-mode FAB-MS, the relevant ions were those for  $\text{Cer}^+$  and  $(\text{CerOH} \cdot \text{H})^+$  at  $m/z$  522/538 Da and 540/556 Da,  $(\text{M} + \text{H})^+$  at  $m/z$  1026 Da and 1042 Da and  $(\text{M} + 2\text{H}^+ - \text{acyl})^+$  at  $m/z$  788 Da and 804 Da (Figs 6c and 8b).

The pseudomolecular ( $\text{M-H}^-$ ) ions of glycosphingolipid component 4 in negative-mode FAB-MS were  $m/z$  1186 Da and 1202 Da, in this case without chloride adducts. The carbohydrate sequence Hex-Hex-Hex-Hex was documented by the ion series at  $m/z$  1024 Da and 1040 Da ( $\text{M-H-Hex}^-$ ), 862 Da and 878 Da ( $\text{M-H-2Hex}^-$ ), 700 Da and 716 Da ( $\text{M-H-3Hex}^-$ ) and ceramide ions at  $m/z$  538 Da and 554 Da (Figs 5d and 8a). The cation of the type  $(\text{M} + 2\text{H}^+ - \text{acyl})^+$  was detected at  $m/z$  950 Da, as well as those at  $m/z$  1188 Da ( $\text{M} + \text{H}^+$ ), 540 Da ( $\text{CerOH} \cdot \text{H}^+$ ) and 522 Da  $\text{Cer}^+$  (Figs 6d and 8b). The phytosphingosine-derived molecular and fragment ions did not apparently desorb under the conditions employed. The relevant fragment ions, from negative- and positive-ion FAB-MS, for the structural analysis of glycosphingolipid components 1–4 are depicted in Table 4.

#### $^1\text{H-NMR}$ spectroscopy

In the one-dimensional  $^1\text{H-NMR}$  of the native glycosphingolipid components 2 and 3 in  $\text{C}^2\text{HCl}_3/\text{C}^2\text{H}_3\text{O}^2\text{H}$  (1:1, by vol.), the hexose resonances are observed in the region 3.0–4.5 ppm, together with intense signals originating from  $\text{C}^2\text{H}_2\text{HOH}$ . In order to resolve these resonances [33], the samples were remeasured in  $\text{C}^2\text{HCl}_3$  following peracetylation. Three groups of resonances showing two or three protons occurred at 5.0–5.4 ppm in the one-dimensional spectra (data not shown). In the HH-COSY of peracetylated glycosphingolipid component 2, two anomeric protons were observed as doublets at 4.40 ppm and 4.451 ppm, with identical coupling

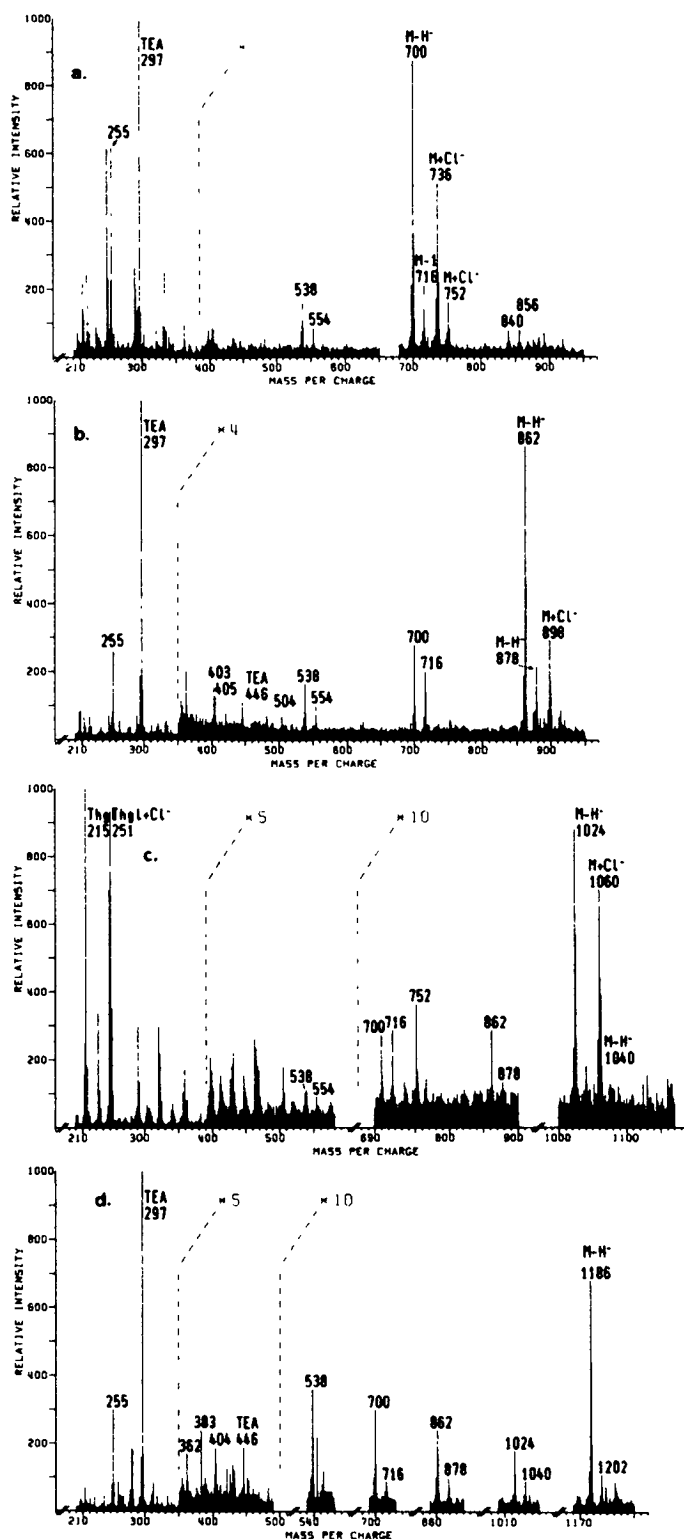


**Fig. 5.** FAB-MS of native neutral glycosphingolipid components 1–4 in the negative-ion mode. (a–d) Negative-ion spectra of components 1–4, respectively. The assignment of ions is indicated in the respective fragmentation pathways (see Fig. 8).

constants of  $^3J_{1,2} = 7.9$  Hz, consistent with a  $\beta$ -anomeric glycosidic linkage (Fig. 9). The C2–C4 protons are all located at 5.0–5.4 ppm (Table 5). The coupling constants for the C1–C4 protons (Table 5) with  $^3J_{3,4} < 3$  Hz are consistent with the sugar residues being galactopyranoses, however, be-

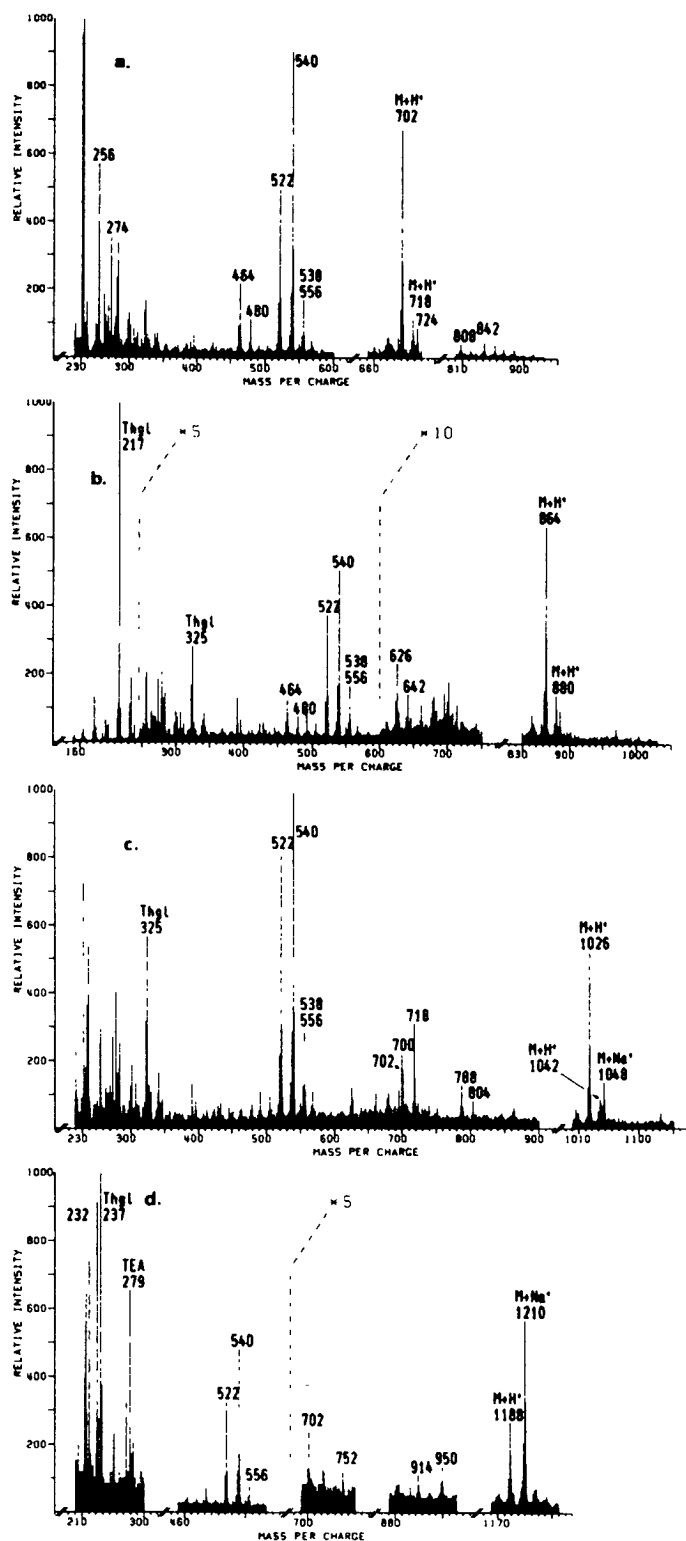


Fig. 6. FAB-MS of native neutral glycosphingolipid components 1–4 in the positive-ion mode. (a–d) Positive-ion spectra of components 1–4. The assignment of ions is indicated in the fragmentation pathways (see Fig. 8).

cause of the small  $^3J_{4,5}$  coupling constant, no assignment of C5H and C6H could be made. From the downfield shifts of the C2H–C4H resonances relative to the native compound, induced by *O*-acetylation, glycosidic substitution at C2, C3 or C4 can be safely excluded. By exclusion, the substitution is

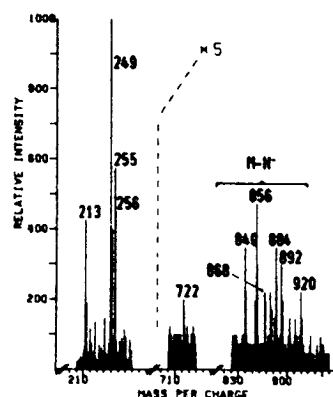


Fig. 7. Negative-ion-mode FAB-MS of reverse-phase-HPTLC-isolated component band 5, derived from glycosphingolipid component 1.

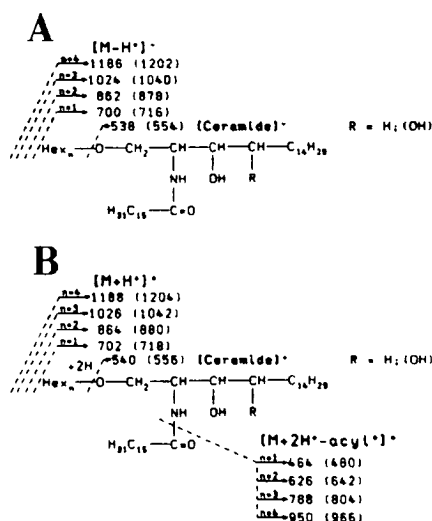


Fig. 8. Fragmentation pathways of neutral glycolipid components 1–4 derived from FAB-MS. (A) Negative-ion mode; (B) positive-ion mode.

located at C6, i.e. <sup>13</sup>Galβ6<sup>1</sup>Galβ1Cer. The NH proton of the peracetylated component 2 at 6.02 ppm can be attributed to a 3,4-*O*-acetylphytosphingosine [34, 35].

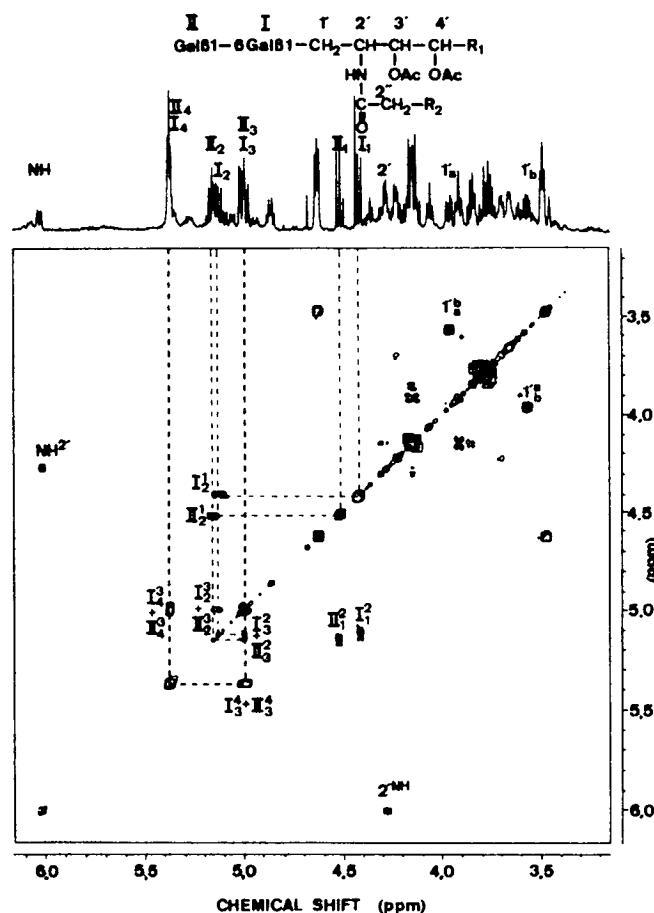
In the HH-COSY of peracetylated glycosphingolipid component 3 (data not shown), analogous chemical shifts and coupling constants were observed (Table 5). The additional carbohydrate moiety, a β-linked galactose, is characterised by an anomeric proton at 4.48 ppm. On the basis of the small differences in chemical shift for the anomeric protons, and because of the missing shift values for C5H and C6H, no unequivocal attribution of individual galactose proton resonances to single galactose units can be made. Again, by exclusion, the proposed structure for component 3 is <sup>13</sup>Galβ6<sup>1</sup>Galβ6<sup>1</sup>Galβ1Cer.

## DISCUSSION

Platyhelminth parasites (Trematoda and Cestoda) depend for survival and propagation on specialized, and possibly unusual, biological properties of their outer tegument cell-surface membranes. Host infection, encounter with mechanical and chemical stress of the host's internal milieu, defence against immune attack and the specific uptake of nutrients, are phenomena suggestive of the existence of specialized mech-

**Table 4.** Relevant molecular and fragment ions of native glycosphingolipid components 1–4 from negative- and positive-ion FAB-MS.

Glyco- sphingolipid component	<i>m/z</i> of molecular and fragment ions								
	negative-mode					positive mode			
	[M–H] <sup>–</sup>	[M–H–Hex] <sup>–</sup>	[M–H–2Hex] <sup>–</sup>	[M–H–3Hex] <sup>–</sup>	[Cer–O] <sup>–</sup>	[M+H] <sup>+</sup>	[M+2H <sup>+</sup> –acyl] <sup>+</sup>	[CerOH·H] <sup>+</sup>	[Cer] <sup>+</sup>
	Da								
1	700/716	538/554	—	—	538/554	702/718	464/480	540/556	522/538
2	862/878	700/716	538/554	—	538/554	864/880	626/642	540/556	522/538
3	1024/1040	862/878	700/716	538/554	538/554	1026/1042	788/804	540/556	522/538
4	1186/1202	1024/1040	862/878	700/716	538/554	1188/—	950/—	540/—	522/—

**Fig. 9.** Contour display of HH-COSY in the absolute-value mode of peracetylated, neutral-glycolipid component 2 (downfield area 3.2–6.2 ppm; for experimental details, see Materials and Methods). The attribution of the proton signals to GalI or GalII is not based on spectroscopic evidence, but serves exclusively for the labelling of Gal residues.

anisms serving these purposes. For a functional participation in such mechanisms, the glycolipids anchored in the outer leaflet of the cell-surface membrane, while orienting their hydrophilic head-group carbohydrates towards the external medium, are ideally located at the lipid-penetration barrier of the membrane and in a strategically favoured position for interactions with the aqueous environment.

The presence of glycolipids in multicellular parasites has been reported: *Hymenolepis diminuta* and *Hymenolepis citelli* [36], *Echinococcus granulosus* and *Moniezia benedeni* [37],

**Table 5.** Chemical shifts and coupling constants ( $^3J_{\text{HH}}$ ) for neutral glycolipid components 2 and 3 from metacestodes of *T. crassiceps*. The attribution of proton signals to GalI, GalII or GalIII is not based on spectroscopic evidence, but serves exclusively for the labelling of Gal residues.  $^3J$  values are shown in parentheses.

Com- ponent	Pro- ton	$\delta$ ( $^3J$ )			
		Gal $\beta$ 1 III	6Gal $\beta$ 1 II	6Gal $\beta$ 1 I	1 Ceramide R e. T.
ppm (Hz)					
2	C1	—	4.51 (C2H, 7.9)	4.40 (C2H, 7.9)	1a, 3.97
	C2	—	5.15 (C3H, 9.0)	5.12 (C3H, 9.0)	1b, 3.58
	C3	—	4.99 (C4H, 2.9)	4.99 (C4H, 2.9)	2, 4.28
	C4	—	5.37	5.37	NH, 6.02
3	C1	4.51 (C2H, 7.9)	4.481 (C2H, 7.9)	4.41 (C2H, 7.9)	1a, 3.97
	C2	5.1	5.1	5.11	1b, 3.58
	C3	4.99	4.99	4.99	2, 4.27
	C4	5.37	5.37	5.37	NH, 6.03

*Spirometra mansonoides* [38], *Schistosoma mansoni* [39, 40] and *Onchocerca gibsoni* [41]. In most of these studies, a large number of glycolipid components have been detected by chromatographic techniques. For example, an earlier investigation of cestode lipids showed the presence of five TLC-separable glycolipids from metacestodes of *T. crassiceps* and the claim of 14 different monosaccharide constituents detected in these compounds [42]; however, this observation has not been substantiated in this publication. Except for more detailed data on the structure of ceramide monohexoside (CMH; GalCer and GlcCer) from *Echinococcus multilocularis* [43], CDH (GalNAc $\beta$ 4GlcCer) from *S. mansoni* [44], and CMH (GalCer) and CDH (LacCer) from *S. mansonoides* [38], no complete structural information on helminth higher glycosphingolipids is presently available. Therefore, in order to characterise further glycosphingolipids of platyhelminth parasites and study their putative role in the maintenance of the host-parasite relationship, a systematic investigation of the glycolipids of the cestode, *T. crassiceps* and related species have been initiated [13, 45]. In these reports, we showed the glycolipids of *T. crassiceps* to be separable by normal-phase silica-gel TLC into groups of bands which superficially corresponded in their migration properties to the series of glycosphingolipids: CMH, CDH, CTH, ceramide tetrahexoside



(CTetH). It is now evident (this publication) that this banding within groups, a phenomenon well known for glycosphingolipids of vertebrate origin, in the case of the parasite glycolipids is also clearly related to differences in the respective ceramide composition, whilst groups of TLC bands of glycosphingolipids are distinguished from one another by differences in the size of the carbohydrate moiety. Under the TLC conditions employed, no heterogeneity of the ceramide residue influencing migration is observed with the neutral fraction *C. vicina* glycosphingolipids used as standards [46].

Analyses of the ceramide constituents of *T. crassiceps* neutral-fraction glycosphingolipids, isolated by reverse-phase TLC, indicate that, in the noticeable absence of octadecaphosphing-4-enine (sphingosine), a major discriminating contribution to the TLC banding phenomenon, is made by the two  $C_{18}$  sphingoids, sphinganine (dihydrosphingosine) and 4-hydroxysphinganine (phytosphingosine). The ceramide-bound-fatty-acid distribution of the glycosphingolipid components 1–4 was documented by both capillary GC and FAB-MS in the negative- and positive-ion modes. The former technique showed the predominance of very-long-chain fatty acids, i.e. 26:0, 28:0 and docosanoic acid (30:0; Fig. 3), while the latter indicated palmitic acid as the dominant fatty acid linked to dihydrosphingosine (as the main component) and phytosphingosine (as a major component), and only traces of higher homologues (Figs 5 and 6). The simplest explanation for this discrepancy in the expression of ceramide-linked fatty acids is that by enrichment of component band M5 through reverse-phase HPTLC, the long-chain moieties can be observed (Fig. 7). This still does not explain the almost exclusive detection of palmitic acid in component bands M1 and M3 by FAB-MS analysis (data not shown). A second possibility for the non-detection of long-chain fatty acids by FAB-MS is that of incomplete desorption from the liquid matrix (thioglycerol or triethanolamine), possibly induced by aggregation.

In contrast, structural elucidation of the carbohydrate moieties from the four groups of TLC bands isolated from *T. crassiceps* neutral-fraction glycosphingolipids has revealed their respective homogeneity. The glycosphingolipid groups contain  $\beta$ -D-galactopyranose or  $\alpha$ -D-galactopyranose as the sole sugar, alone as the CMH Gal $\beta$ 1Cer, or substituted at C6 as the CDH Gal $\beta$ 6Gal $\beta$ 1Cer, CTH Gal $\beta$ 6Gal $\beta$ 6Gal $\beta$ 1Cer and CTetH as Gal $\beta$ 6Gal $\beta$ 6Gal $\beta$ 6Gal $\beta$ 1Cer and Gal $\alpha$ 4Gal $\beta$ 6Gal $\beta$ 6Gal $\beta$ 1Cer. These glycosphingolipids obviously form a biogenetically related series of structures of identical constitution, comparable to those isolated by Matsubara and Hayashi in a series of investigations on the marine snails *Turbo cornutus* [14], *Chlorostoma argyrostoma turbinatum* and *Monodonta labio* [15], as well as *Haliotis japonica*; all these species belonging to the order Archaeogastropoda (Mollusca). In contrast to the  $\beta$ 1–6 linkage of the snail glycosphingolipids, a glycolipid of the marine sponge, *Halichondria japonica* (Spongia: Desmospongia) contains an  $\alpha$ 1–4-linked galactose, Gal $\alpha$ 4Gal < [47].

To name biogenetically related oligogalactosyl saccharides, the designation Gala-4 and Gala-6 series have been recommended earlier [15]. However, in order to avoid confusion of numbers with widely different meanings in abbreviation connotations, the use of gala (Ga for [Gal $\alpha$ 4Gal $\alpha$ ]<sub>n</sub>-Gal $\beta$ 1Cer), neogala (nGa for [Gal $\beta$ 6Gal $\beta$ 6]<sub>n</sub>-Gal $\beta$ 1Cer) and isogala (iGa for [Gal $\alpha$ 6Gal $\alpha$ ]<sub>n</sub>-Gal $\beta$ 1Cer) could be adopted. As well as these glycosphingolipid oligosaccharides consisting solely of galactose, a number of glycolipids from other carbohydrate series exist which also contain oligomeric galactose

units. Amongst these are the globo-series (Gb) glycosphingolipids, III<sup>3</sup>(Gal $\alpha$ 3Gal $\alpha$ 3Gal $\alpha$ -)Gb<sub>3</sub>Cer of rat intestine [48] and PC12 pheochromocytoma cells [49], and the sialoganglio-series (Gg) ganglioside, IV<sup>3</sup>(Gal $\alpha$ 3Gal $\beta$ 3Gal $\alpha$ -), II<sup>3</sup>NeuAc-Gg<sub>4</sub>Cer from muscle [50] and nervous tissue of the frog [51].

In conclusion, and as a motive for the future, we have attempted to define the two physicochemical properties of glycosphingolipids which we consider may impart particular advantages to the plasma membrane (tegument) of cestodes, as exemplified by the neogala glycosphingolipids of *T. crassiceps* metacestodes. Firstly, the rigidity and stability of the plasma membrane, as influenced by ceramide-induced hydrogen bonding, may involve and be increased by the galactose residue located at the lipid-hexose linkage region and the hydroxylated long-chain base, phytosphingosine. In this regard, the observation that, of the monosaccharides investigated in glyceroglycolipid model membranes, the galactose head group conferred the highest stability, may be of significance [52]. Secondly, the  $\beta$ 1–6 linkage of neogala oligosaccharide chains bestows a greater flexibility, as opposed to glycosidic bonds in other positions of the various carbohydrate series of the glycosphingolipids. Our eventual aim is to be able to establish a verifiable working hypothesis as to the putative physiological significance of *T. crassiceps* glycosphingolipids as functional plasma-membrane glycoconjugates. Nishimura et al. [53] have recently published a study on the neutral-fraction glycosphingolipids of the cestode, *Metrolia sthes coturnix*.

The authors wish to express their appreciation of the excellent technical assistance of Werner Mink and Siegfried Kühnhardt (University of Giessen) and Manfred Plüger (University of Bonn). The investigations received partial support from the *Fonds der Chemischen Industrie* (to H. W.) and the *Deutsche Forschungsgemeinschaft* (*Sonderforschungsbereich 272, Teilprojekt B1* to R. G.).

## REFERENCES

1. Sastry, P. S. (1974) *Adv. Lipid Res.* 12, 251–310.
2. Laine, R. A., Hsieh, T. C.-Y. & Lester, R. L. (1980) *ACS Symp. Ser.* 128, 65–78.
3. Stults, C. L. M., Sweeley, C. C. & Macher, B. A. (1989) *Methods Enzymol.* 179, 167–211.
4. Ishizuka, I. & Yamakawa, T. (1985) *New Compr. Biochem.* 10, 101–198.
5. Hakomori, S., Igarashi, Y., Nojiri, H., Bremer, E., Hanai, N. & Nore, G. A. (1990) in *Trophic factors and the nervous system* (Horrocks, L. A., ed.) pp. 135–158. Raven Press, New York.
6. Nojiri, H., Stroud, M. & Hakomori, S. (1991) *J. Biol. Chem.* 266, 4531–4537.
7. Hannun, Y. & Bell, R. (1989) *Science* 243, 500–507.
8. Nagai, Y. & Sakakibara, K. (1991) *Adv. Exp. Med. Biol.* 152, 425–438.
9. Gillard, B. K., Heath, J. P., Thurmon, L. T. & Marcus, D. M. (1991) *Exp. Cell. Res.* 192, 433–444.
10. Simmons, K. & van Meer, G. (1988) *Biochemistry* 27, 6197–6202.
11. Hakomori, S. (1984) *Annu. Rev. Immunol.* 2, 103–126.
12. Freeman, R. S. (1962) *Can. J. Zool.* 40, 969–990.
13. Baumeister, S., Dennis, R. D., Kunz, J., Wiegandt, H. & Geyer, E. (1992) *Mol. Biochem. Parasitol.* 53, 53–62.
14. Matsubara, T. & Hayashi, A. (1981) *J. Biochem. (Tokyo)* 89, 645–650.
15. Matsubara, T. & Hayashi, A. (1986) *J. Biochem. (Tokyo)* 99, 1401–1408.
16. Dennis, R. D., Geyer, R., Egge, H., Menges, H., Stirm, S. & Wiegandt, H. (1985) *Eur. J. Biochem.* 146, 51–58.

17. Gazzotti, G., Sonnino, S. & Ghidoni, R. (1984) *J. Chromatogr.* **315**, 395–400.
18. Carter, H. E. & Hirschberg, C. B. (1968) *Biochemistry* **7**, 2296–2300.
19. Gaver, R. C. & Sweeley, C. C. (1965) *J. Am. Oil Chem. Soc.* **42**, 294–298.
20. Hanfland, P. (1975) *Chem. Phys. Lipids* **15**, 105–124.
21. Williams, M. A. & McCluer, R. H. (1980) *J. Neurochem.* **35**, 266–269.
22. Kuhn, R. & Wiegandt, H. (1963) *Chem. Ber.* **96**, 866–880.
23. Geyer, R., Geyer, H., Kühnhardt, S., Mink, W. & Stirm, S. (1983) *Anal. Biochem.* **33**, 197–207.
24. Björndal, H., Hellerqvist, C. G., Lindberg, B. & Svensson, S. (1970) *Angew. Chem.* **82**, 643–674.
25. Jansson, P. E., Kenne, L., Liedgren, H., Lindberg, B. & Lönngren, J. (1976) *Univ. Stockholm Chem. Commun.* **8**, 1–75.
26. Paz Parente, J., Cardon, P., Leroy, Y., Montreuil, J., Fournet, B. & Ricart, G. (1985) *Carbohydr. Res.* **141**, 41–47.
27. Uda, Y., Li, S.-C., Li, Y.-T. & McKibbin, J. M. (1977) *J. Biol. Chem.* **252**, 5194–5200.
28. Chou, D. K. H., Ilyas, A. A., Evans, J. E., Costello, C., Quarles, R. H. & Jungalwala, F. B. (1986) *J. Biol. Chem.* **261**, 11 717–11 725.
29. Egge, H. & Peter-Katalinic, J. (1987) *Mass Spectrom. Rev.* **6**, 331–393.
30. Aue, W., Bartholdi, E. & Ernst, E. E. (1976) *J. Chem. Phys.* **64**, 2229–2246.
31. Dennis, R. D., Geyer, R., Egge, H., Peter-Katalinic, J., Li, S.-C., Stirm, S. & Wiegandt, H. (1985) *J. Biol. Chem.* **260**, 5370–5375.
32. Peter-Katalinic, J. & Egge, H. (1990) *Methods Enzymol* **193**, 713–733.
33. Dabrowski, U., Egge, H. & Dabrowski, J. (1983) *Arch. Biochem. Biophys.* **224**, 254–260.
34. Röder, B., Dabrowski, J., Dabrowski, U., Egge, H., Peter-Katalinic, J., Schwarzmann, G. & Sandhoff, K. (1990) *Chem. Phys. Lipids* **53**, 85–89.
35. Dabrowski, J., Dabrowski, U., Hanfland, P., Kordowicz, M. & Hull, W. E. (1986) *Magn. Reson. Chem.* **24**, 729–733.
36. Harrington, G. W. (1965) *Exp. Parasitol.* **17**, 287–295.
37. Hrzenjak, T. & Ehrlich, I. (1976) *Vet. Arh.* **46**, 9–15.
38. Singh, B. N., Beach, D. H., Walenga, R. W., Mueller, J. F. & Holz, G. G. (1987) in *Molecular paradigms for eradicating helminthic parasites* (MacInnis, A. J., ed.) vol. 60, pp. 493–506, Alan R. Liss Inc.
39. Maloney, M. D., Semprevivo, L. H. & Coles, G. C. (1990) *Int. J. Parasitol.* **20**, 1091–1093.
40. Weiss, J. B., Magnani, J. L. & Strand, M. (1986) *J. Immunol.* **136**, 4275–4282.
41. Maloney, M. D. & Semprevivo, L. H. (1991) *Parasitol. Res.* **77**, 294–300.
42. Mills, G. L., Taylor, D. C. & Williams, J. F. (1981) *Comp. Biochem. Physiol.* **69B**, 553–557.
43. Persat, F., Bouhours, J. F., Mojon, M. & Petavy, A. F. (1990) *Mol. Biochem. Parasitol.* **41**, 1–6.
44. Makaaru, C., Damian, R. T., Smith, D. F. & Cummings, R. D. (1992) *J. Biol. Chem.* **267**, 2251–2257.
45. Kunz, J., Baumeister, S., Dennis, R. D., Küytz, B., Wiegandt, H. & Geyer, E. (1991) *Parasitol. Res.* **77**, 443–447.
46. Helling, F., Dennis, R. D., Weske, B., Nores, G. A., Peter-Katalinic, J., Dabrowski, U., Egge, H. & Wiegandt, H. (1991) *Eur. J. Biochem.* **200**, 409–421.
47. Hayashi, A., Nishimura, Y. & Matsubara, T. (1991) *Biochim. Biophys. Acta* **1083**, 179–186.
48. Breimer, M. E., Hansson, G. C., Karlsson, K.-A. & Leffler, H. (1982) *J. Biol. Chem.* **257**, 557–568.
49. Ariga, T., Suzuki, M., Yu, R. K., Simoda, I., Kitagawa, H., Inagaki, F. & Miyatake, T. (1989) *J. Biol. Chem.* **264**, 1516–1521.
50. Ohashi, M., Yasuda, Y. & Tanaka, N. (1988) in *Third Rinsho-ken international conference—biomedical significance of glycolipids* (Yamakawa, T., ed.) p. 12, Tokyo Metropolitan Institute of Medical Science.
51. Ohashi, M. (1980) *J. Biochem. (Tokyo)* **88**, 583–589.
52. Hinz, H.-J., Kuttentrich, H., Meyer, R., Renner, M., Fründ, R., Koynova, R., Boyanov, A. I. & Tenchov, B. G. (1991) *Biochemistry* **30**, 5125–5138.
53. Nishimura, K., Suzuki, A. & Kino, H. (1991) *Biochim. Biophys. Acta* **1086**, 141–150.

Copyright of European Journal of Biochemistry is the property of Blackwell Publishing Limited and its content may not be copied or emailed to multiple sites or posted to a listserv without the copyright holder's express written permission. However, users may print, download, or email articles for individual use.